Journal of Nuclear Materials 385 (2009) 68–71

Contents lists available at ScienceDirect

Journal of Nuclear Materials

journal homepage: www.elsevier.com/locate/jnucmat

Density-functional study of Zr-based actinide alloys

Alex Landa [a,*], Per Söderlind [a], Patrice E.A. Turchi [a], L. Vitos [b], A. Ruban [b]

[a] Lawrence Livermore National Laboratory, Livermore, CA 94551, USA
[b] Royal Institute of Technology, SE-10044 Stockholm, Sweden

A B S T R A C T

Density-functional formalism is applied to study the phase equilibria in the U–Zr system. The obtained ground-state properties of the γ (bcc) and δ (C32) phases are in good agreement with experimental data. The decomposition curve for the γ-based U–Zr solutions is calculated. We argue that stabilization of the δ-UZr_2 phase relative to the α-Zr (hcp) structure is due to an increase of the Zr d-band occupancy that occurs when U is alloyed with Zr.

1. Introduction

Zr-based actinide alloys, particularly U–Pu–Zr, proved to be very promising fuels for liquid metal fast breeder reactors because of their advantage in view of superior performance, reactor safety, and fuel cycle economics [1]. The main goal of fast breeder reactors is to achieve a so-called 'high burn-up' fissioning all types of transuranic elements thus providing an appropriate solution to spent fuel recycling and complete transmutation of long-lived minor actinides (Np, Am, and Cm) [2].

It was established [3] that the U–Zr system is characterized by the complete solubility of the body centered cubic high-temperature phases, γ-U and β-Zr, that is usually referred to in phase diagrams by 'γ-phase' solid solutions. Below $T \approx 995$ K, these solutions separate into a relatively flat miscibility gap, which ranges from 10 to 40 at.% of Zr, and spans about 30 K below the critical point. The intermediate δ-phase is formed on cooling from the γ-phase around UZr_2 stoichiometry with the homogeneity range from 63 to 82 at.% Zr [4].

The γ-U–Zr phase plays an important role in metallurgical reactions that occur during the nuclear burn-up [5–7]. That is why in this paper we present results of *ab initio* calculations of the decomposition curve for the γ-U–Zr alloys. Another remarkable feature is the δ-UZr_2 phase, which solidifies in a modified C32 (AlB_2)-type structure. It is well known that the high-temperature Zr-based solid solutions may transform into the so-called metastable ω-phase at low temperatures [8], which can also be stabilized from the α (hcp) phase of Zr under compression [8,9]. According to X-ray and neutron diffraction analysis of the UZr_2 compound [4,10], Zr atom occupies the 'Al' position of the hexagonal cell and a random mixture of U and Zr atoms occupies the 'B' positions. Ogawa et al. [11] suggested that the δ-UZr_2 phase could be regarded as the ω-phase solid solution that is stabilized against the α-Zr (hcp) structure by addition of U due to increase of Zr d-band occupancy. Here we present results of calculations verifying the hypothesis [11] for the δ-UZr_2 stabilization.

In our calculations we employ three complementary computational techniques: (i) scalar-relativistic Green's function technique based on the Korringa–Kohn–Rostoker (KKR) method within the atomic-sphere approximation (ASA), (ii) the scalar-relativistic exact muffin-tin orbital method (EMTO), and (iii) the all-electron full-potential linear muffin-tin orbital method (FPLMTO) that accounts for all relativistic effects.

2. Computational details

The calculations we have referred to as KKR–ASA are performed using the scalar-relativistic Green's function technique based on the KKR method within the atomic-sphere approximation [12–15]. For the electron exchange and correlation energy functional, the generalized gradient approximation (GGA) is adopted [16]. Integration over the Brillouin zone is performed using the special k-point technique [17]. The equilibrium density of the U–Zr system is obtained from a Murnaghan [18] fit.

In order to treat compositional disorder the KKR–ASA method is combined with the coherent potential approximation (CPA) [19]. The ground-state properties of the random U–Zr alloys are obtained from KKR–ASA–CPA calculations with the Coulomb screening potential and energy [20–22]. The screening constants are determined from supercell calculations using the locally self-consistent Green's function method [23]. The effective cluster interactions, used in Monte Carlo (MC) simulations, are obtained from the screened generalized-perturbation method [20,21,24].

Though the KKR–ASA formalism is well suited to treat close-packed structures it could produce a significant error when being

* Corresponding author. Tel.: +1 925 424 3523; fax: +1 925 422 2851.
E-mail address: landa1@llnl.gov (A. Landa).

0022-3115/$ - see front matter © 2008 Elsevier B.V. All rights reserved.
doi:10.1016/j.jnucmat.2008.09.029

applied to 'open' structures, e.g., C32. That is why we use a Green's function technique, based on the EMTO formalism, in present calculations, which is not limited by geometrical restrictions imposed by the ASA.

The EMTO calculations are performed using scalar-relativistic Green's function technique based on the improved screened KKR method [25,26]. The total energy is obtained from the full charge-density technique [27] and GGA is used for the electron exchange and correlation approximation. EMTO is combined with the CPA for calculation of the total energy of chemically random alloy.

For the elemental metals, the most accurate and fully relativistic calculations are performed using an all-electron approach where the relativistic effects, including spin-orbit coupling, are accounted for. Although unable to model disorder in the CPA sense it provides important information for the metals, and also serves to confirm the CPA calculations mentioned above. For this purpose we use a version of the FPLMTO [28]. As in the case of the KKR–ASA and EMTO methods, GGA is used for the electron exchange-correlation approximation. A special quasi-random structure (SQS) method was used to treat the compositional disorder within the FPLMTO formalism [29].

3. Ground-state properties and decomposition curve of the γ-U–Zr solid solutions

Fig. 1 shows the results of KKR–ASA–CPA calculations of the heat of formation of the γ-U–Zr solid solutions at $T = 0$ K. The heat of formation shows a positive deviation from the Vegard's law that agrees well with the existence of a miscibility gap in the U–Zr phase diagram. Notice that the calculated heat of formation of the γ-U–Zr solid solutions is in excellent agreement with data extracted from the experimental phase diagram by the use of CALPHAD methodology [30], which suggests a robustness of the *ab initio* approach. For comparison, we also show the heats of formation for the $U_{75}Zr_{25}$, $U_{50}Zr_{50}$, and $U_{25}Zr_{75}$ bcc alloys calculated within the FPLMTO–SQS technique.

We performed MC calculations of the decomposition curve for the γ-U–Zr solid solutions. The MC simulations are performed using the Metropolis algorithm [31] for a 1728-site simulation box ($12 \times 12 \times 12$) with periodic boundary conditions. Fig. 2 displays the calculated temperature of decomposition of the γ-$U_{1-c}Zr_c$ alloys within the wide range of composition. This curve has a maximum that is located somewhere between 20 and 30 at.% of Zr. This maximum matches relatively well the location of the maximum on the experimental miscibility gap (~30 at.% Zr) also shown in the figure.

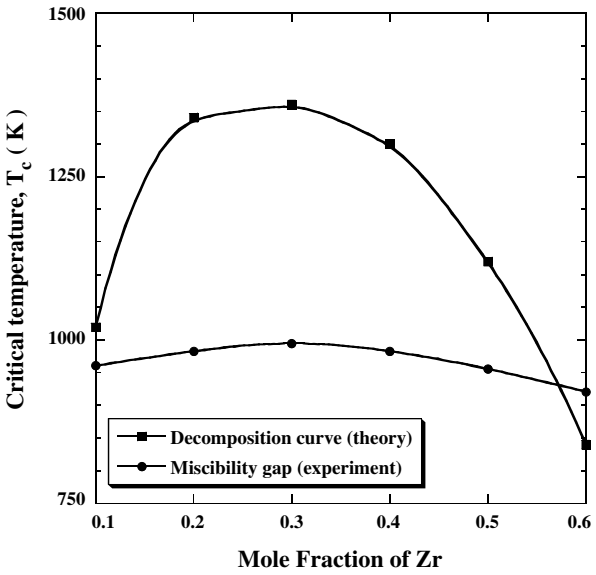

Fig. 2. Temperature of decomposition of the γ-U–Zr alloys. Experimental data on the miscibility gap are taken from Ref. [32].

4. Ground-state properties of the δ-UZr_2 compound

The C32 (AlB_2) structure has two non-equivalent types of sublattice with three atoms per unit cell: sublattices of 'Al-' (one site) and 'B-' (two sites) types. It is believed that in the δ-UZr_2 compound Zr atoms occupy the Al-type position (0, 0, 0) of the hexagonal cell, and a random mixture of U and Zr atoms occupies the B-type positions (2/3, 1/3, 1/2) and (1/3, 2/3, 1/2). To confirm that

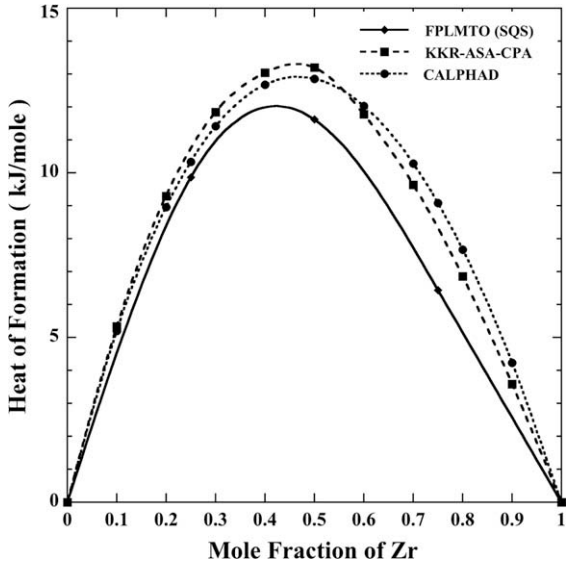

Fig. 1. The heat of formation of the γ-U–Zr alloys ($T = 0$ K).

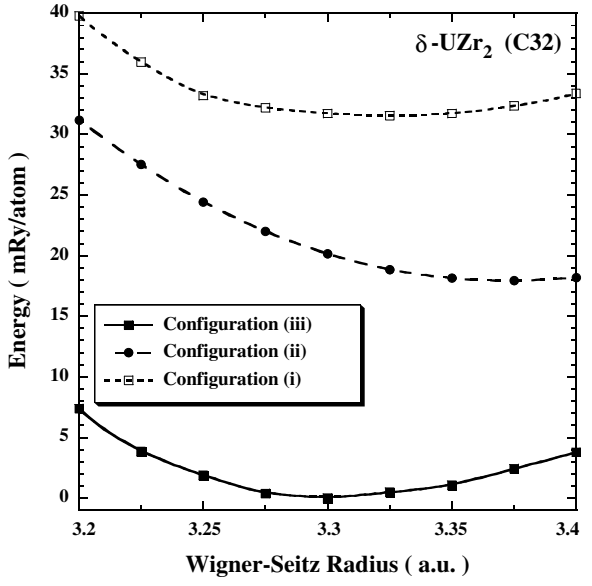

Fig. 3. The total energy of the δ-UZr_2 compound for (i)–(iii) configurations (see text) as a function of the Wigner–Seitz radius. The equilibrium energy of the 'partially' order configuration (iii) is used as the reference point and is set equal to zero.

this arrangement is the ground-state configuration of the δ-UZr_2 compound, we performed EMTO calculations of the equilibrium lattice constant for three atomic configurations of the C32 structure: (i) random distribution of U and Zr atoms on each of the three sites (the $U_{1/3}Zr_{2/3}$ 'disordered' alloy); (ii) 'complete' ordering with U atoms occupying the Al-type sublattice and Zr atoms occupying the B-type sublattice; (iii) 'partial' ordering that corresponds to experimental observation described in Section 1. Fig. 3 shows the total energy of the δ-UZr_2 compound as a function of the Wigner–Seitz radius. One can see that two types of ordering, 'complete' and 'partial', are energetically favorable in comparison with the disordered configuration, however, the configuration (iii) is one that has the lowest total energy. We have also calculated the enthalpy of formation ($E^{C32}_{UZr_2}$) of the δ-UZr_2 compound. Present calculations reveal $E^{C32}_{UZr_2}$ = −6.29 kJ/mol that is in fair agreement with experimental measurements of −4.0 kJ/mol at T = 298 K [33,34].

5. Stability of the δ-phase in the U–Zr system

It is well established that under compression zirconium metal undergoes the following phase transformations: α-Zr (hcp) → ω-Zr (C32) → β-Zr (bcc) [8,9,35–37]. According to the present FPLMTO calculations, the α → ω and ω → β phase transitions in Zr take place at 33 and 268 kbar, respectively, which are in a good accord with experimental measurements [8,9,35–37].

Fig. 4(a) shows results of FPLMTO calculations of the s-, p-, and d-band occupations in α-Zr as a function of the Wigner–Seitz radius (pressure). As pressure increases, the occupation of the d-band goes up due to a loss of the s- and p-band electrons. In Fig. 4(b) we show the structural-energy difference obtained from canonical bands [38] as a function of d-band filling. One can see that as the d-band occupation increases under compression, hcp transforms to C32 and then to bcc.

Next, we discuss the analogies with the U–Zr system. Fig. 5 has two parts. The upper part shows how the d-band occupation of α-Zr changes under compression and the transition region (full black) spans between the lower and upper experimental bounds, 21 and 85 kbar [8,37], of the α → ω transformation. The hatched patch of the upper part of the plot shows the pressure region of the certain ω-phase stability in pure Zr. The lower part of this plot shows how the d-band occupation changes as a function of an increase in U composition in the U–Zr system. The hatched part of this part of the plot spans within the range of the homogeneity of the δ-U–Zr phase (18–37 at.% U [4]). One can see that at the upper pressure border of the α → ω phase transition range in pure Zr (∼85 kbar) its d-occupation almost reaches the same value as it has when composition of U, alloyed with α-Zr, reaches the value (∼18 at.%, [4]) when the δ-UZr_2 phase starts to form. Thus the present calculations confirm the hypothesis [11] that stabilization of the δ-UZr_2

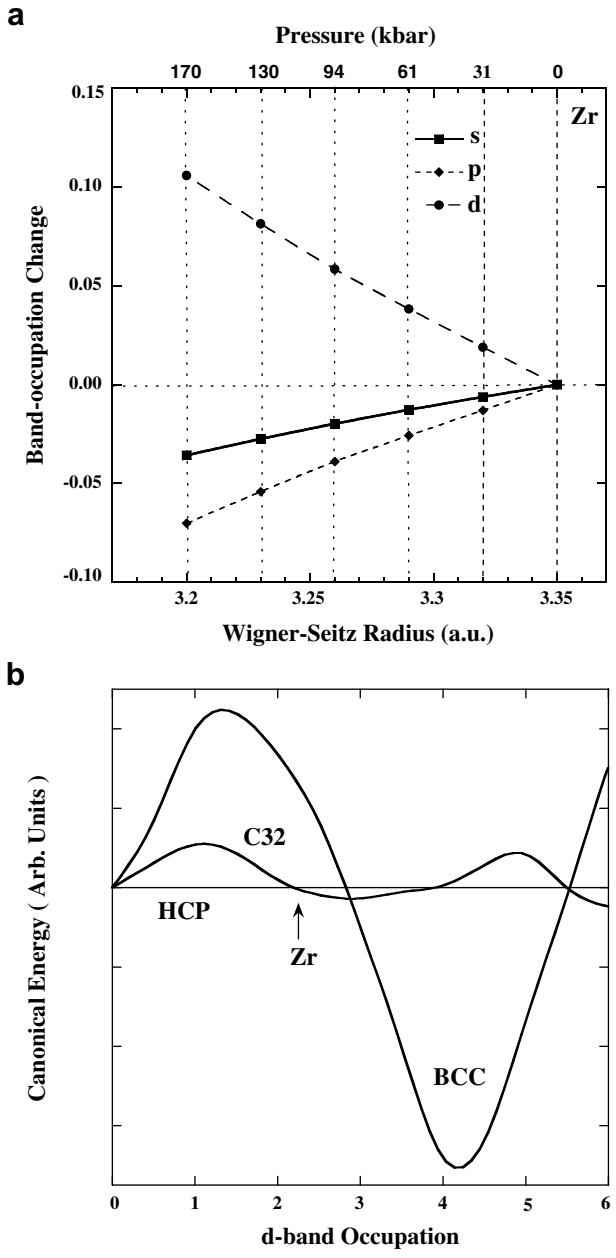

Fig. 4. The change in band occupations in α-Zr under compression (a): the energy difference obtained from canonical d-bands calculations as a function of d-band occupancy (b): the hcp phase is used as the reference point and is set equal to zero.

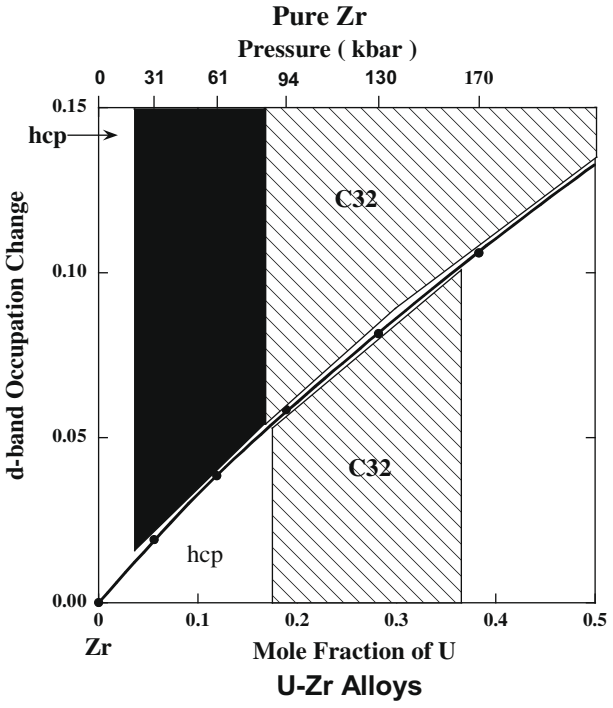

Fig. 5. Comparison of d-band occupancy in α-Zr as a function of compression with d-band occupancy in the U–Zr hcp alloys as a function of U concentration.

phase has the same origin as that of the ω-phase in pure Zr under compression, namely, it is induced by an increase in d-band filling.

6. Conclusion

In the present paper *ab initio* results are obtained for U–Zr alloys to understand the effectiveness of first-principles methods in describing actinide alloys. Ground-state properties of the γ-U-Z solid solutions and δ-UZr_2 compound were calculated. Predicted temperature of decomposition of the γ-U–Zr alloys is in a reasonable agreement with the γ-phase miscibility gap. Stabilization of the δ-UZr_2 phase is explained in terms of an increase in d-band occupancy by the addition of U to Zr.

Acknowledgements

This work was performed under the auspices of the US DOE by LLNL under contract DE-AC52-07NA27344.

References

[1] G.L. Hofman, L.C. Walters, T.H. Bauer, Progr. Nucl. Energy (1/2) (1997) 83.
[2] D.D. Keiser Jr., J.B. Kennedy, B.A. Hilton, S.L. Hayes, JOM (1) (2008) 29.
[3] T. Ogawa, T. Iwai, J. Less Common Met. 170 (1991) 101.
[4] M. Akabori, A. Itoh, T. Ogawa, F. Kobayashi, Y. Suzuki, J. Nucl. Mater. 188 (1992) 249.
[5] T. Ogawa, T. Iwai, M. Kurata, J. Less Common Met. 175 (1991) 59.
[6] G.L. Hofman, S.L. Hayes, M.C. Petri, J. Nucl. Mater. 227 (1996) 277.
[7] T. Ogawa, M. Akabori, A. Itoh, T. Ogawa, J. Nucl. Mater. 232 (1996) 125.
[8] S.K. Sikka, Y.K. Vohra, R. Chidambaran, Prog. Mater. Sci. 27 (1982) 245.
[9] H. Xia, A.L. Ruoff, Y.K. Vohra, Phys. Rev. B 44 (1991) 10374.
[10] M. Akabori, T. Ogawa, A. Itoh, Y. Morii, J. Phys.: Condens. Matter 7 (1995) 8249.
[11] T. Ogawa, J.K. Gibson, R.G. Haire, M.M. Gensini, M. Akabori, J. Nucl. Mater. 223 (1995) 67.
[12] O. Gunnarson, O. Jepsen, O.K. Andersen, Phys. Rev. B 27 (1983) 7144.
[13] I.A. Abrikosov, H.L. Skriver, Phys. Rev. B 47 (1993) 16532.
[14] A.V. Ruban, H.L. Skriver, Comput. Mater. Sci. 15 (1999) 119.
[15] N.E. Christensen, S. Satpathy, Phys. Rev. Lett. 55 (1985) 600.
[16] J.P. Perdew, K. Burke, M. Ernzerhof, Phys. Rev. Lett. 77 (1996) 3865.
[17] D.J. Chadi, M.L. Cohen, Phys. Rev. B 8 (1973) 5747;
D.J. Chadi, M.L. Cohen, Phys. Rev. B 39 (1989) 3168.
[18] F.D. Murnaghan, Proc. Natl. Acad. Sci. USA 30 (1944) 244.
[19] J.S. Faulkner, Prog. Mater. Sci. 27 (1982) 1.
[20] A.V. Ruban, H.L. Skriver, Phys. Rev. B 66 (2002) 02420-1.
[21] A.V. Ruban, S.I. Simak, P.A. Korzhavyi, H.l. Skriver, Phys. Rev. B 66 (2002) 024202-1.
[22] A.V. Ruban, S.I. Simak, S. Shallcross, H.L. Skriver, Phys. Rev. B 67 (2003) 214302-1.
[23] I.A. Abrikosov, S.I. Simak, B. Johansson, A.V. Ruban, H.L. Skriver, Phys. Rev. B 56 (1997) 9319.
[24] A.V. Ruban, I.A. Abrikosov, Rep. Prog. Phys. 71 (2008) 046501-1.
[25] L. Vitos, Phys. Rev. B 64 (2001) 014107-1.
[26] L. Vitos, Computational Quantum Mechanics for Materials Engineers: The EMTO Method and Application, Springer, London, 2007.
[27] J. Kollar, L. Vitos, H.L. Skriver, in: H. Dreyssé (Ed.), Electronic Structure and Physical Properties of Solids: The Uses of the LMTO Method, Lecture Notes in Physics, Springer, Berlin, 2000, p. 85.
[28] J.M. Wills, O. Eriksson, M. Alouani, D.L. Price, in: H. Dreyssé (Ed.), Electronic Structure and Physical Properties of Solids: The Uses of the LMTO Method, Lecture Notes in Physics, Springer, Berlin, 2000, p. 148.
[29] A. Zunger, S.H. Wei, L.G. Ferreira, J.E. Bernard, Phys. Rev. Lett. 65 (1990) 353.
[30] P.E.A. Turchi, I.A. Abrikosov, B. Burton, S.G. Fries, G. Grimvall, L. Kauffman, P. Korzhavyi, V. Rao Manga, M. Ohno, A. Pisch, A. Scott, W. Zhang, CALPHAD 31 (2007) 4.
[31] K. Binder, Application of the Monte Carlo Method in Statistical Physics, Springer, Berlin, 1987.
[32] H. Okamoto, J. Phase Equilib. 14 (2) (1993) 267.
[33] K. Nagarajan, R. Babu, C.K. Mathews, J. Nucl. Mater. 203 (1993) 221.
[34] T. Ogawa, J. Nucl. Mater. 209 (1994) 107.
[35] S.A. Ostanin, V.Yu. Trubisin, Phys. Rev. 57 (1998) 13485.
[36] Y. Akahama, M. Kobayashi, H. Kawanura, J. Phys. Soc. Jpn. 60 (1991) 3211.
[37] C.W. Greeff, Model. Simul. Mater. Sci. Eng. 13 (2005) 1015.
[38] H.L. Skriver, Phys. Rev. B 31 (1985) 1909.